Supplementary Information (SI) for CrystEngComm.

Electronic Supplementary Information

3D ED for the localization of cations in potassium exchanged and partially dehydrated nano Y zeolite

Y. M. Chaib Draa[ab], T. Örs[ab], I. Deroche[ab], C. Dejoie[c], J.-L. Paillaud[ab]

[a] Université de Haute-Alsace, Institut de Science des Matériaux de Mulhouse (IS2M), UMR CNRS 7361, 68100 Mulhouse, France
[b] Université de Strasbourg, 67000 Strasbourg, France
[c] European Synchrotron Radiation Facility, 71 avenue des Martyrs 38000 Grenoble, France.

TABLE OF CONTENT

1 Experimental procedure

1.1 Synthesis and cationic exchange of nano faujasite K-Y

Nano Y zeolite was synthesised according to the protocol of Borel et al. The reaction gel had the following molar composition: 9.4 SiO_2: 0.2 Al_2O_3: 4.95 Na_2O: 150 H_2O. It was prepared as follows. Sodium hydroxide was dissolved in water with stirring, followed by the addition of sodium aluminate. The mixture was heated to 50°C in an oil bath with stirring at 350 rpm for 45 minutes until completely dissolved, then cooled to 4°C in an ice bath. Ludox AS-40 was then added slowly to the solution, stirring at 500 rpm. The gel formed was left at room temperature for 17 hours with stirring at 500 rpm. The PP bottle containing the gel was placed in an oven at 90°C for 8 hours, followed by 5 cycles of centrifugal washing with distilled water until a pH of less than 9-10 was obtained. Finally, the zeolite was dried in an oven at 100°C overnight. Nano Y zeolite in sodium form was exchanged with KCl to obtain exchanged K-Y zeolite, the exchange protocol was as follows: nano Y zeolite was placed in a solution of KCl (1M), then stirred for 24 hours at 300 rpm. After shaking, the exchanged zeolite was washed with deionised water. This exchange process was repeated 3 times to maximise the exchange rate.

1.2 Scanning Electron Microscopy and Energy Dispersive X-ray spectroscopy

Scanning electron microscopy (SEM) images and energy dispersive X-ray spectroscopy (EDX) analysis were measured on a JEOL JSM-7900F scanning electron microscope equipped with a Bruker Quantax analyser system made of two XFlash 6-30 detectors. Prior to analysis, the sample was coated with a thin film of carbon using a Baltec SCD004 coater.

1.3 Powder X-ray diffraction (PXRD) measurements

The PXRD pattern of the hydrated nano faujasite K-Y zeolite was acquired using a Malvern-Panalytical Empyrean Alpha1 diffractometer (Debye-Scherrer geometry) equipped with a single Ge symmetrical monochromator (Johansson assembly) emitting Cu Kα1 radiation (λ = 1.5406 Å). The diffractometer featured a capillary spinner stage and a PIXcel^{1D} silicon strip direct detector (active length = 3.3482° 2θ). The dataset was collected over a 2θ range of 5° to 90°, using a step size of 0.007° and an acquisition time of 2000 seconds per step. The total data collection time was 29 hours, 19 minutes, and 40 seconds. A Le Bail refinement was subsequently performed using the GSAS-II[1] software.

High-resolution powder diffraction data of the dehydrated sample, were collected at the ID22 beamline (European Synchrotron Radiation Facility), using the thirteen-crystal multianalyzer stage.[2] The wavelength of 0.354417(1) Å was calibrated using a Si NIST 640c standard. The sample was packed in a 1-mm diameter quartz capillary, and mounted on a dedicated cell for in situ dehydration. Dehydration was carried out in two steps. First, the cell connected to a turbo vacuum pump was placed for one night in an oven at 150 °C. Then, it was mounted on a custom-made spinner that allows a 30° rocking during data collection to improve powder average while being connected to the vacuum system. Before collecting the data, a second dehydration step was carried out in situ using an Oxford Cryosystems Cryostream 1000 plus (150°C for 1 hour). A temperature of 150 °C was chosen to achieve effective dehydration without causing complete dehydration. Data were collected after going back to room temperature, keeping the cell connected to the vacuum system.

---

[1] B. H. Toby and R. B. Von Dreele, *J. Appl. Crystallogr.*, 2013, **46**, 544-549.

[2] A. Fitch, C. Dejoie, E. Covacci, G. Confalonieri, O. Grendal, L. Claustre, P. Guillou, J. Kieffer, W. de Nolf, S. Petitdemange, M. Ruat and Y. Watier, *J. Synchrotron Radiat.*, 2023, **30**, 1003-1012.

1.4 Thermogravimetric analysis

The thermogravimetric analysis was carried out on a TG Mettler Toledo STARe apparatus under airflow, with a heating rate of 5 °C min^{-1} and in the 30 to 800 °C temperature range. 31.3588 mg of the nano K-Y sample previously water saturated in a moisture atmosphere (saturated NH_4Cl solution) was placed in an alumina crucible inside the furnace. Following this measurement cycle, a second run on an identical empty crucible (referred to as a “blank”) was performed to subtract the effects of buoyancy and the thermal capacity of the sample, ensuring more accurate interpretation of the mass loss data.

1.5 3D ED data collection and TEM image collection

The precession electron diffraction (PED) measurements were conducted using a CM200 TEM (Philips, Eindhoven The Netherlands) equipped with a Digistar P2010 (NanoMEGAS, Brussels, Belgium) precession system. Data were recorded by a side entry Phurona CMOS (EMSIS, Munster, Germany) camera (12M pixel model). An acceleration voltage of 200kV was applied, and the camera length was set at 1200 mm. the sample was ground and deposited directly on a carbon-coated Cu gird. In precession tomography mode, diffraction was consecutively acquired by manually tilting (without the use of automated acquisition software) the same crystal along the α-axis of the single-tilt sample holder. The tilting step size was 1°, and the crystal was rotated in an angular range of −52° to +35°. During rotation, the electron beam was deviated to minimize the exposure time of the sample. The TEM was operated under a vacuum of 10^{-5} Pa. The estimated total electron dose used during data collection (including the additional dose from regularly re-centring the crystal) is 0.8 e Å^{-2}.

2 Data analysis

2.1 Data Reduction and integration steps (3D ED)

Data reduction and integration using PETS2.0 software involves processing the raw 3D ED electron diffraction data, indexing the diffraction patterns, extracting the intensities and integrating them into the data set. PETS2.0 automates these processes, ensuring accurate data reduction and improving the reliability of the structural model.

2.2 Structural solution and localisation of cations (3D ED)

The reflection intensities were extracted from PETS2.0 after the optimization of the orientation angles. The resulting *hkl* file was imported to Jana2020 and the crystal structure obtained from the charge-flipping algorithm applied to the extracted intensities directly provided the atomic positions of silicon and oxygen atoms of the nano FAU framework. This is used as the initial model for the structure refinement.

This processes required additional steps, including successive difference Fourier map calculations, to determine the positions of the extra framework spices.

First steps kinematic refinement: this is the standard method used in crystallography. In this type of refinement, the calculations are based mainly on the amplitudes of the scattered intensities, without taking into account the dynamical interactions between the electrons and atoms of the crystal. This makes it possible to quickly obtain an approximate structural model.

Then a dynamical refinement: This method is used in crystallography to fit a structural model to experimental data, taking dynamic effects into account. Unlike kinematic refinement, which simplifies by neglecting these effects, dynamic refinement takes the mobility of the atoms in the crystal, the thickness of the single crystal and its orientation. This provides a more accurate and realistic model of the crystal structure by taking into account the dynamic interactions between the electrons in the beam and the single crystal.

2.3 Rietveld refinement of nano faujasite K-Y based on high-resolution powder diffraction data after in situ dehydration

The Rietveld refinement was performed using the GSAS-II[1] software. First, a Le Bail refinement allowed us to determine the background and profile parameters and to refine the unit cell parameters. Then, the atomic coordinates of the whole framework of nano K-Y zeolite determine by the present 3D ED study (i.e., Si,Al and O atoms) were used as the starting model for the Rietveld refinement. Soft restraints were placed on the bond lengths and angles of the framework (T−O = 1.65(5) Å and O−T−O = 109.5(40)°). To determine a proper scale factor, only the high angle window $25 < 2\theta < 40$ °(2θ)) was taken into account,[3] and then the whole pattern (0.5−40 °(2θ)) was used for the following steps. All atomic displacement parameters were refined isotropically. After refinement of the framework, the calculated Fourier difference maps revealed scattering electronic densities inside the sodalite cage and to the position of sites I and II unambiguously attributable to the potassium cations and also to the remaining water molecules inside the sodalite cage. After convergence, the resulting crystal and Rietveld refinement data for nano faujasite K-Y are listed in Table S5. The atomic parameters (coordinates, occupancies, and atomic displacement parameters) and selected bonds and angles, are provided in Table S6 and S7, respectively.

---

[3] L. B. McCusker, R. B. Von Dreele, D. E. Cox, D. Louer and P. Scardi, *J. Appl. Crystallogr.*, 1999, **32**, 36-50.

Table S1: Crystal and structural refinement data for nano faujasite K-Y, with two distinct columns highlighting the values that differ between kinematical and dynamical refinements.

	Dynamical refinement	Kinematical refinement
Refined empirical formula	$Si_{134,40}$ $Al_{57,60}$ $O_{389.03}K_{56.28}$	$Si_{134,40}$ $Al_{57,60}$ $O_{384}K_{53.21}$
Formula weight	13753.4	13553
Temperature/K	293	
Crystal system	Cubic	
Space group	$Fd\bar{3}m$ (227)	
a (Å)	24.96(1)	24.95(1)
V (Å^3)	15556.5(2)	15528.6(2)
Z	1	
Density (g/cm^3)	1.4681	1.4493
F(000)	2399.534	2362.077
Crystal size (nm)	~200 × ~285	
Data collection mode	Precession assisted 3D ED	
Source (wavelength)	Electrons (λ = 0.02508 Å)	
2θ range for data collection (°)	0.05 to 1.01	
Index ranges	$-32 \leq h \leq 33$, $-28 \leq k \leq 30$, $-28 \leq l \leq 33$	$-33 \leq h \leq 31$, $-33 \leq k \leq 28$, $-30 \leq l \leq 28$
Reflections collected	26476	1083
Independent reflections	3235	393
Data coverage for sinθ/λ = 0.6 Å^{-1}	0.98	1
Restraints/contraints/parameters	0 / 6 / 121	0 / 4 / 23
g_{max}, R_{Sg}	1.6/0.66	
Largest differences peak and hole (e Å^{-3})	0.17, -0.15	0.53, -0.39
Avg./Min/Max Crystal thickness (Å^{-3})	818 / 351 / 1586	/
Goodness-of-fit on F^2	Obs: 3.36 / All: 1.46	3.46/5.66
Final R values [I > 3σ(I)] (%)	11.00 / 19.65	22.86/43.94
Final R values [all data] (%)	43.21 / 24.04	34.26/45.11

Crystallographic data after the dynamical refinement have been deposited at CCDC under deposition numbers 2452355 and can be obtained from https://www.ccdc.cam.ac.uk/structures/. Other data supporting this article have been included as part of the ESI.†

Table S2: Atomic positions, isotropic displacement parameters (e.s.d. in brackets) of nano faujasite K-Y (3D ED, kinematical refinement).

Atom	Wyck.[a]	Site	s.o.f.[b]	x/*a*	y/*b*	z/*c*	U [Å^2][c]
Si	192i	1	0.7[d]	0.3048(2)	0.1259(2)	0.2145(2)	0.0190(14)
Al	192i	1	0.3[d]	0.3048(2)	0.1259(2)	0.2145(2)	0.0190(14)
O1	96h	..2		0.3580(4)	0.1080(4)	1/4	0.040(4)
O2	96g	..m		0.3204(5)	0.1811(3)	0.1811(3)	0.029(3)
O3	96g	..m		0.2533(4)	0.1396(5)	0.2533(4)	0.039(4)
O4	96g	..m		0.2851(5)	0.0762(4)	0.1738(4)	0.035(4)
K1	16c	.-3m	0.39(4)	0	0	0	0.006(11)
K1'	32e	.3m	0.47(3)	0.1747(7)	0.0753(7)	0.1747(7)	0.069(13)
K2	32e	.3m		0.5012(3)	0.5012(3)	0.7488(3)	0.056(4)

Table S3: Atomic positions, isotropic displacement parameters (e.s.d. in brackets) of nano faujasite K-Y (3D ED, dynamical refinement).

Atom	Wyck.[a]	Site	s.o.f.[b]	x/*a*	y/*b*	z/*c*	U [Å^2][c]
Si	192i	1	0.7[d]	0.03577(6)	0.30396(5)	0.12439(6)	0.0187(4)
Al	192i	1	0.3[d]	0.03577(6)	0.30396(5)	0.12439(6)	0.0187(4)
O1	96h	..2		0	0.35754(10)	0.14243(10)	0.0453(13)
O2	96g	..m		0.07037(10)	0.31610(14)	0.07039(10)	0.0346(11)
O3	96g	..m		-0.00299(10)	0.25299(10)	0.11119(13)	0.0355(12)
O4	96g	..m		0.07556(11)	0.28558(16)	0.17444(11)	0.0560(13)
K(I)	16c	.-3m	0.481(1)	0	0	0	0.011(2)
K(I')	32e	.3m	0.518(1)	0.07826(14)	0.07826(14)	0.07826(14)	0.0750(9)
K(II)	32e	.3m		0.25092(8)	0.25092(8)	0.25092(8)	0.0750(9)
Ow1	32e	.3m	0.1570(3)	0.1841(10)	0.1841(10)	0.1841(10)	0.0750(9)

Table S4: Selected geometric parameters (Å, °, e.s.d. in brackets) for nano faujasite K-Y (3D ED, dynamical refinement).

Si,Al—O1	1.671 (3)	K(I)—K(I')	3.384 (3)
Si,Al—O2	1.630 (3)	K(I)—K(I')^{iii}	3.384 (3)
Si,Al—O3	1.632 (3)	K(I')—K(I')^{ii}	3.300 (5)
Si,Al—O4	1.661 (3)	K(I')—K(I')^{iv}	3.300 (5)
Si,Al—K(1)^{i}	3.528 (2)	K(I')—K(I')^{i}	3.300 (5)
Si,Al—K(1')^{i}	3.663 (4)	K(I')—Ow1^{ii}	2.68 (3)
Si,Al—K(II)^{ii}	3.518 (2)	K(I')—Ow1^{iv}	2.68 (3)
O3—K(II)^{ii}	2.800 (4)	K(I')—Ow1^{i}	2.68 (3)
O4—K(I)^{i}	2.812 (3)	K(II)—Ow1	2.89 (3)
O4—K(I')^{i}	2.843 (5)		

O1—Si,Al—O2	110.94 (16)	O4^{xi}—K(I)—O4^{xiii}	88.50 (10)
O1—Si,Al—O3	111.23 (13)	O4^{xii}—K(I)—O4^{xiii}	88.50 (10)
O1—Si,Al—O4	109.77 (16)	O4^{i}—K(I')—O4^{ix}	87.25 (12)
O2—Si,Al—O3	107.00 (18)	O4^{i}—K(I')—O4^{x}	87.25 (12)
O2—Si,Al—O4	110.88 (16)	O4^{i}—K(I')—Ow(I')^{iv}	84.6 (5)
O3—Si,Al—O4	106.92 (18)	O4^{i}—K(I')—Ow1^{ii}	168.7 (6)
Si,Al—O1—Si,Al^{v}	135.85 (17)	O4^{i}—K(I')—Ow1^{i}	84.6 (5)
Si,Al—O2—Si,Al^{vi}	147.4 (2)	O4^{ix}—K(I')—O4^{x}	87.25 (12)
Si,Al—O3—Si,Al^{vii}	152.1 (2)	O4^{ix}—K(I')—Ow1^{iv}	168.7 (6)
Si,Al—O4—Si,Al^{viii}	145.4 (3)	O4^{ix}—K(I')—Ow1^{ii}	84.6 (5)
O4^{i}—K(I)—O4^{ix}	88.50 (10)	O4^{ix}—K(I')—Ow1^{i}	84.6 (5)
O4^{i}—K(I)—O4^{x}	88.50 (10)	O4^{x}—K(I')—Ow1^{iv}	84.6 (5)
O4^{i}—K(I)—O4^{xi}	91.50 (10)	O4^{x}—K(I')—Ow1^{ii}	84.6 (5)
O4^{i}—K(I)—O4^{xii}	91.50 (10)	O4^{x}—K(I')—Ow1^{i}	168.7 (6)
O4^{i}—K(I)—O4^{xiii}	180	Ow(I')^{ii}—K(I')—Ow1^{iv}	102.4 (8)
O4^{ix}—K(I)—O4^{x}	88.50 (10)	Ow(I')^{ii}—K(I')—Ow1^{i}	102.4 (8)
O4^{ix}—K(I)—O4^{xi}	91.50 (10)	Ow(I')^{iv}—K(I')—Ow1^{i}	102.4 (8)
O4^{ix}—K(I)—O4^{xii}	180	O3^{ii}—K2—O3^{xiv}	92.10 (9)
O4^{ix}—K(I)—O4^{xiii}	91.50 (10)	O3^{ii}—K2—O3^{xv}	92.10 (9)
O4^{x}—K(I)—O4^{xi}	180	O3^{xiv}—K2—O3^{xv}	92.10 (9)
O4^{x}—K(I)—O4^{xii}	91.50 (10)	K(I')^{ii}—Ow1—K(I')^{iv}	76.1 (7)
O4^{x}—K(I)—O4^{xiii}	91.50 (10)	K(I')^{ii}—Ow1—K(I')^{i}	76.1 (7)
O4^{xi}—K(I)—O4^{xii}	88.50 (10)	K(I')^{iv}—Ow1—K(I')^{i}	76.1 (7)

Symmetry codes: (i) x, −y+1/4, −z+1/4; (ii) −x+1/4, y, −z+1/4; (iii) −y, −x, −z; (iv) −x+1/4, −y+1/4, z; (v) −x, −z+1/2, −y+1/2; (vi) z, y, x; (vii) −y+1/4, −x+1/4, z; (viii) −z+1/4, y, −x+1/4; (ix) −z+1/4, x, −y+1/4; (x) −y+1/4, −z+1/4, x; (xi) y−1/4, −x, z−1/4; (xii) −x, z−1/4, y−1/4; (xiii) z−1/4, y−1/4, −x; (xiv) −z+1/4, −x+1/4, y; (xv) y, −z+1/4, −x+1/4.

Table S5: Crystal structure and Rietveld refinement data for dehydrated nano faujasite K-Y, obtained from Rietveld refinement of high-resolution synchrotron diffraction data.

Sample	nano KY
Refined chemical formula	$Al_{0.6}K_{0.593}O_{4.04}Si_{1.4}$
Space group	$Fd\bar{3}m$ (# 227)
λ (Å), synchrotron	0.354417(1)
Data collection temperature (K)	293
a (Å)	24.88160(3)
V (Å^3)	15404.04(6)
Z	96
Computing Rietveld software	GSAS-II[1]
No. of data points, 2θ range (°2θ) (step (° 2θ)	26346, 0.5-40.0, 0.0015
No. of contributing reflections	2744
No. of structural variables	22
No. of profile parameters	6
Total number of constraints, restraints (bonds, angles)	11, 11 (5, 6)
Bond restraints: mean(wt·$\sum(\Delta/\sigma)^2$) [a]	0.02(2) [b]
Angle restraints: mean(wt·$\sum(\Delta/\sigma)^2$) [a]	0.79(4) [b]
$(\Delta/\sigma)_{max}$	0.006
$(\Delta/\sigma)_{mean}$	0.0006
Goodness of fit all	4.074
R_p, wR_p [c]	0.0436, 0.0403
R_B, wR_B [c]	0.0788, 0.0936
R_F, R_F^2 [c]	0.0573, 0.0663
wR_{exp} [c]	0.01
Index ranges	$1 \le h \le 48$, $0 \le k \le 33$, $0 \le l \le 27$
Largest differences peak and hole (e Å^{-3})	1.427, -1.146

[a] σ = 0.05 Å (Si−O) for the zeolite framework bond distances, σ = 3° for the O−Si−O angles. [b] Inside parentheses are the weight factors. [c] The definition of these residual values are given in GSAS-II reference paper.[1]

Table S6: Atomic positions and isotropic displacement parameters (e.s.d. in parentheses) of nano dehydrated faujasite K-Y, obtained from Rietveld refinement of high-resolution synchrotron diffraction data.

Atom	**Wyck.**[a]	**Site**	**s.o.f.**[b]	**x/*a***	**y/*b***	**z/*c***	**U [Å^2]**[c]
Si	192i	1	0.7[d]	0.03589(3)	0.30515(3)	0.12425(3)	0.00863(3)
Al	192i	1	0.3[d]	0.03589(3)	0.30515(3)	0.12425(3)	0.00863(3)
O1	96h	..2		0	0.35768(5)	0.14232 (5)	0.0158(2)
O2	96g	..m		0.06766(6)	0.31992(8)	0.0676(6)	0.0158(2)
O3	96g	..m		−0.00211(6)	0.25211(6)	0.11074(8)	0.0158(2)
O4	96g	..m		0.07778(6)	0.28694(9)	0.17222(6)	0.0158(2)
K(I)	16c	.-3m	0.373(3)	0	0	0	0.0237(3)
K(I'a)	32e	.3m	0.470(5)	0.1511(7)	0.1511(7)	0.1511(7)	0.0237(3)
K(I'b)	32e	.3m	0.121(4)[e]	0.0719(1)	0.0719(1)	0.0719(1)	0.0237(3)
Ow1	32e	.3m	0.121(4)[e]	0.0872(5)	0.0872(5)	0.0872(5)	0.0500[f]
K(II)	32e	.3m		0.24986(3)	0.24986(3)	0.24986(3)	0.0237(3)

[a] Multiplicity and Wyckoff letters. [b] s.o.f. for site occupancy factor. [c] Atoms with the same isotropic temperature factor are constrained to be equal. [d] s.o.f. fixed after the EDX analysis. [e] The s.o.f. of K(I'b) and Ow1 were constrained to be equal, a removal of this constraint led to close values. [f] Due to a strong correlation between the s.o.f. and the isotropic displacement parameters of this site, the U_{iso} was fixed to a reasonable value.

Table S7: Selected geometric parameters (Å, °, e.s.d. in brackets) for dehydrated faujasite K-Y, obtained from Rietveld refinement of high-resolution synchrotron diffraction data.

Si,Al—O1	1.6455 (11)	K(I'a)—O4$^{\mathrm{i}}$	2.716 (2)
Si,Al—O2	1.6562 (8)	K(I'a)—O4$^{\mathrm{ii}}$	2.716 (2)
Si,Al—O3	1.6578 (10)	K(I'a)—O4$^{\mathrm{v}}$	2.716 (3)
Si,Al—O4	1.6482 (11)	K(I'b)—O4$^{\mathrm{i}}$	3.105 (2)
K(I)—O4$^{\mathrm{i}}$	2.8872 (12)	K(I'b)—O4$^{\mathrm{ii}}$	3.105 (2)
K(I)—O4$^{\mathrm{ii}}$	2.8872 (12)	K(I'b)—O4$^{\mathrm{v}}$	3.105 (12)
K(I)—O4$^{\mathrm{iii}}$	2.8872 (12)	K(I'b)—Ow1	2.754 (12)
K(I)—O4$^{\mathrm{iv}}$	2.8872 (12)	K(II)—O2$^{\mathrm{viii}}$	2.9467 (14)
K(I)—O4$^{\mathrm{v}}$	2.8872 (12)	K(II)—O2$^{\mathrm{ix}}$	2.9467 (14)
K(I)—O4$^{\mathrm{vi}}$	2.8872 (12)	K(II)—O2$^{\mathrm{x}}$	2.9467 (14)
K(I'a)—O3$^{\mathrm{i}}$	3.097 (2)	K(II)—O3$^{\mathrm{viii}}$	2.753 (2)
K(I'a)—O3$^{\mathrm{v}}$	3.097 (2)	K(II)—O3$^{\mathrm{x}}$	2.7529 (19)
K(I'a)—O3$^{\mathrm{vii}}$	3.097 (2)	K(II)—O3$^{\mathrm{xi}}$	2.7529 (19)

O1—Si,Al—O2	108.36 (8)	O4$^{\mathrm{iii}}$—K(I)—O4$^{\mathrm{xiii}}$	91.29 (6)
O1—Si,Al—O3	112.23 (7)	O4$^{\mathrm{viii}}$—K(I)—O4$^{\mathrm{xiii}}$	91.29 (7)
O2—Si,Al—O3	106.05 (10)	O4$^{\mathrm{iii}}$—K(I)—O4$^{\mathrm{vi}}$	88.71 (6)
O1—Si,Al—O4	111.32 (8)	O4$^{\mathrm{iv}}$—K(I)—O4$^{\mathrm{vi}}$	88.71 (7)
O2—Si,Al—O4	112.01 (8)	O4$^{\mathrm{v}}$—K(I)—O4$^{\mathrm{vi}}$	180
O3—Si,Al—O4	106.78 (11)	O4$^{\mathrm{i}}$—K(I'a)—O4$^{\mathrm{ii}}$	95.98 (6)
Si,Al—O1—Si,Al$^{\mathrm{xii}}$	136.77 (8)	O4$^{\mathrm{i}}$—K(I'a)—O4$^{\mathrm{v}}$	95.98 (7)
Si,Al—O2—Si,Al$^{\mathrm{xiii}}$	139.67 (12)	O4$^{\mathrm{ii}}$—K(I'a)—O4$^{\mathrm{v}}$	95.98 (6)
Si,Al—O3—Si,Al$^{\mathrm{xiv}}$	150.08 (13)	O4$^{\mathrm{i}}$—K(I'b)—O4$^{\mathrm{ii}}$	81.07 (6)
Si,Al—O4—Si,Al$^{\mathrm{ix}}$	147.18 (16)	O4$^{\mathrm{i}}$—K(I'b)—O4$^{\mathrm{v}}$	81.1 (2)
O4$^{\mathrm{i}}$—K(I)—O4$^{\mathrm{iv}}$	91.29 (6)	O4$^{\mathrm{ii}}$—K(I'b)—O4$^{\mathrm{v}}$	81.1 (2)
O4$^{\mathrm{ii}}$—K(I)—O4$^{\mathrm{iv}}$	180	O4$^{\mathrm{i}}$—K(I'b)—Ow1	131.4 (3)
O4$^{\mathrm{iii}}$—K(I)—O4$^{\mathrm{iv}}$	88.71 (6)	O4$^{\mathrm{ii}}$—K(I'b)—Ow1	131.4 (3)
O4$^{\mathrm{i}}$—K(I)—O4$^{\mathrm{v}}$	88.71 (6)	O4$^{\mathrm{v}}$—K(I'b)—Ow1	131.4 (4)
O4$^{\mathrm{ii}}$—K(I)—O4$^{\mathrm{v}}$	88.71 (7)	O2$^{\mathrm{viii}}$—K(II)—O2$^{\mathrm{ix}}$	110.46 (4)
O4$^{\mathrm{iii}}$—K(I)—O4$^{\mathrm{v}}$	91.29 (6)	O2$^{\mathrm{viii}}$—K(II)—O2$^{\mathrm{x}}$	110.46 (4)
O4$^{\mathrm{iv}}$—K(I)—O4$^{\mathrm{v}}$	91.29 (7)	O2$^{\mathrm{ix}}$—K(II)—O2$^{\mathrm{x}}$	110.46 (6)
O4$^{\mathrm{i}}$—K(I)—O4$^{\mathrm{vi}}$	91.29 (6)	O3$^{\mathrm{viii}}$—K(II)—O3$^{\mathrm{x}}$	92.31 (4)
O4$^{\mathrm{ii}}$—K(I)—O4$^{\mathrm{vi}}$	91.29 (7)	O3$^{\mathrm{viii}}$—K(II)—O3$^{\mathrm{xi}}$	92.31 (4)
O4$^{\mathrm{iii}}$—K(I)—O4$^{\mathrm{vi}}$	88.71 (6)	O3$^{\mathrm{x}}$—K(II)—O3$^{\mathrm{xi}}$	92.31 (3)

Symmetry codes: (i) −z+1/4, x, −y+1/4; (ii) −z+1/4, −y+1/4, x; (iii) z−1/4, −x, y−1/4; (iv) z−1/4, y−1/4, −x; (v) −y+1/4, −z+1/4, x; (vi) y−1/4, z−1/4, −x; (vii) x, −y+1/4, −z+1/4; (viii) −z+1/4, −x+1/4, y; (ix) −z+1/4, y, −x+1/4; (x) y, −z+1/4, −x+1/4; (xi) −x+1/4, y, −z+1/4; (xii) −x, −z+1/2, −y+1/2; (xiii) z, y, x; (xiv) −y+1/4, −x+1/4, z.

Table S8: Average charge compensating K^+ cations distribution per unit cell and per cationic site simulated for faujasite K-Y of composition $K_{56}Si_{136}Al_{56}O_{384}$ in the dehydrated form, varying with water molecules loading.

H_2O / u.c.		I	I′	II	II′	III	III′	Other
0	K^+ nb	10.0	8.9	26.0	1.2	2.8	4.8	2.3
	s.o.f.	0.63	0.28	0.81	0.04	0.06	0.05	
5	K^+ nb	9.0	9.1	29.3	0.0	1.3	5.1	2.2
	s.o.f.	0.56	0.29	0.92	0.0	0.03	0.05	
15	K^+ nb	10.0	7.9	26.7	1.1	0.9	6.5	2.9
	s.o.f.	0.63	0.25	0.83	0.03	0.02	0.07	
30	K^+ nb	7.3	7.1	25.8	2.6	1.4	7.7	4.1
	s.o.f.	0.46	0.22	0.81	0.08	0.03	0.08	
45	K^+ nb	8.0	6.4	26.9	1.6	0.8	7.8	4.5
	s.o.f.	0.50	0.20	0.84	0.05	0.02	0.08	
60	K^+ nb	7.0	8.2	27.7	0.8	0.3	8.6	3.4
	s.o.f.	0.44	0.26	0.87	0.02	0.01	0.09	
80	K^+ nb	7.0	6.9	29.4	0.7	0.4	9.6	2
	s.o.f.	0.44	0.21	0.92	0.02	0.01	0.10	
100	K^+ nb	6.9	7.2	29.6	0.0	0.4	9.1	2.8
	s.o.f.	0.43	0.22	0.93	0.00	0.01	0.09	

Figure S1: A SEM image of nano faujasite K-Y.

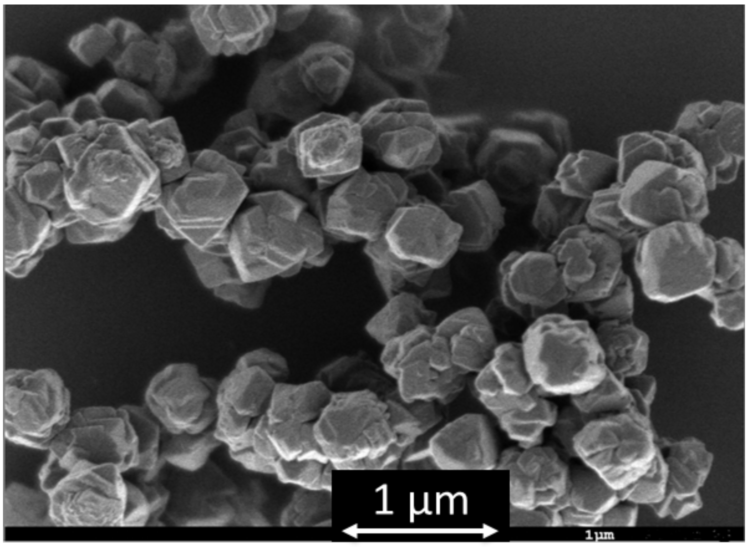

Figure S2: TEM image of the measured nano faujasite K-Y crystal.

Figure S3: Energy dispersive X-ray spectroscopy (EDX) analyses of nano faujasite K-Y. Analysis method: Phi-Rho-Z Calibrated elements: Si, Al,O on albite, K on KBr.

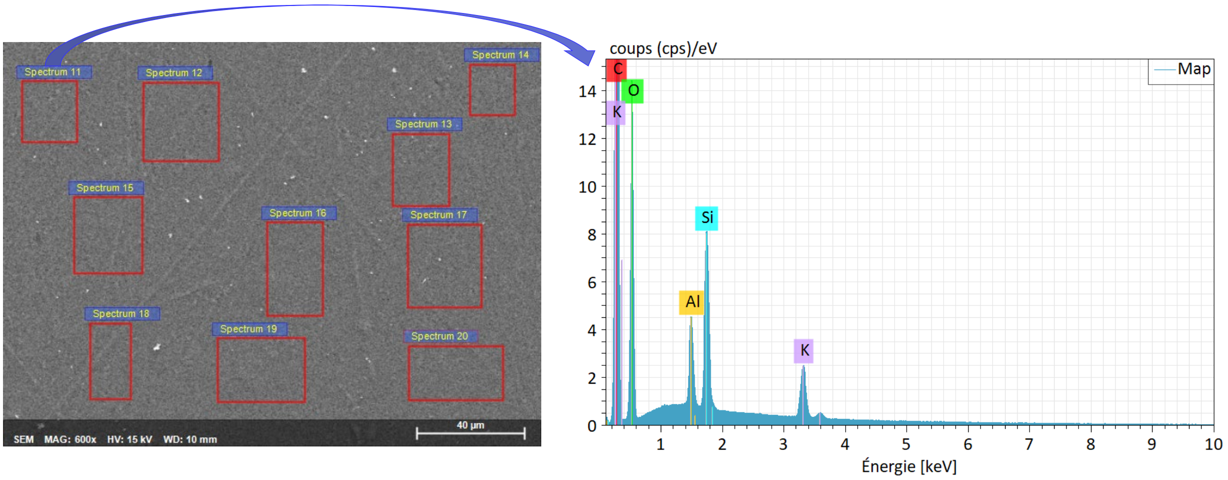

Atomic composition (%)				
Spectrum	**O**	**Al**	**Si**	**K**
Spectrum 11	63.32	8.61	19.71	8.37
Spectrum 12	63.47	8.56	19.57	8.4
Spectrum 13	63.33	8.58	19.65	8.45
Spectrum 14	63.24	8.61	19.72	8.34
Spectrum 15	63.47	8.55	19.61	8.39
Spectrum 16	63.42	8.59	19.55	8.41
Spectrum 17	63.42	8.62	19.55	8.41
Spectrum 18	63.28	8.6	19.75	8.4
Spectrum 19	63.38	8.58	19.64	8.38
Spectrum 20	63.35	8.57	19.67	8.42
Mean	**63.37**	**8.59**	**19.64**	**8.4**
Sigma	0.08	0.02	0.07	0.03
SigmaMean	0.03	0.01	0.02	0.02

Atomic composition (%) calculated for $Si_{134,4}\ Al_{57,6}\ O_{384}K_{57.6}(H_2O)_{40}$				
	O	**Al**	**Si**	**K**
	62.95	**8.55**	**19.95**	**8.55**

Figure S4: Le Bail fit of the hydrated nano faujasite K-Y (λ = 1.5406 Å). The angular range 47.75-90° in 2*θ* (°) is magnified by a factor 18.

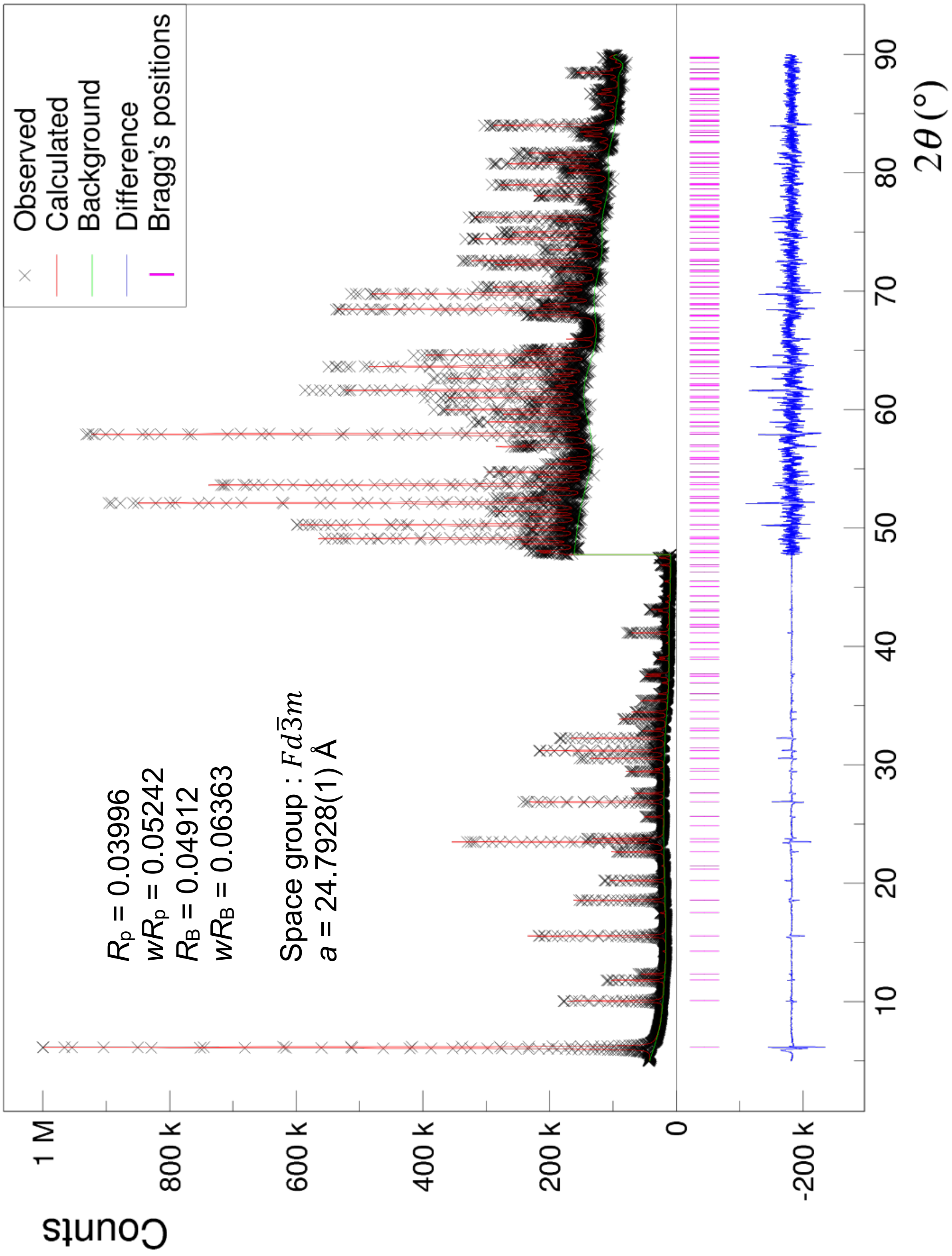

Figure S5: Thermogravimetric curve of the hydrated nano faujasite K-Y.

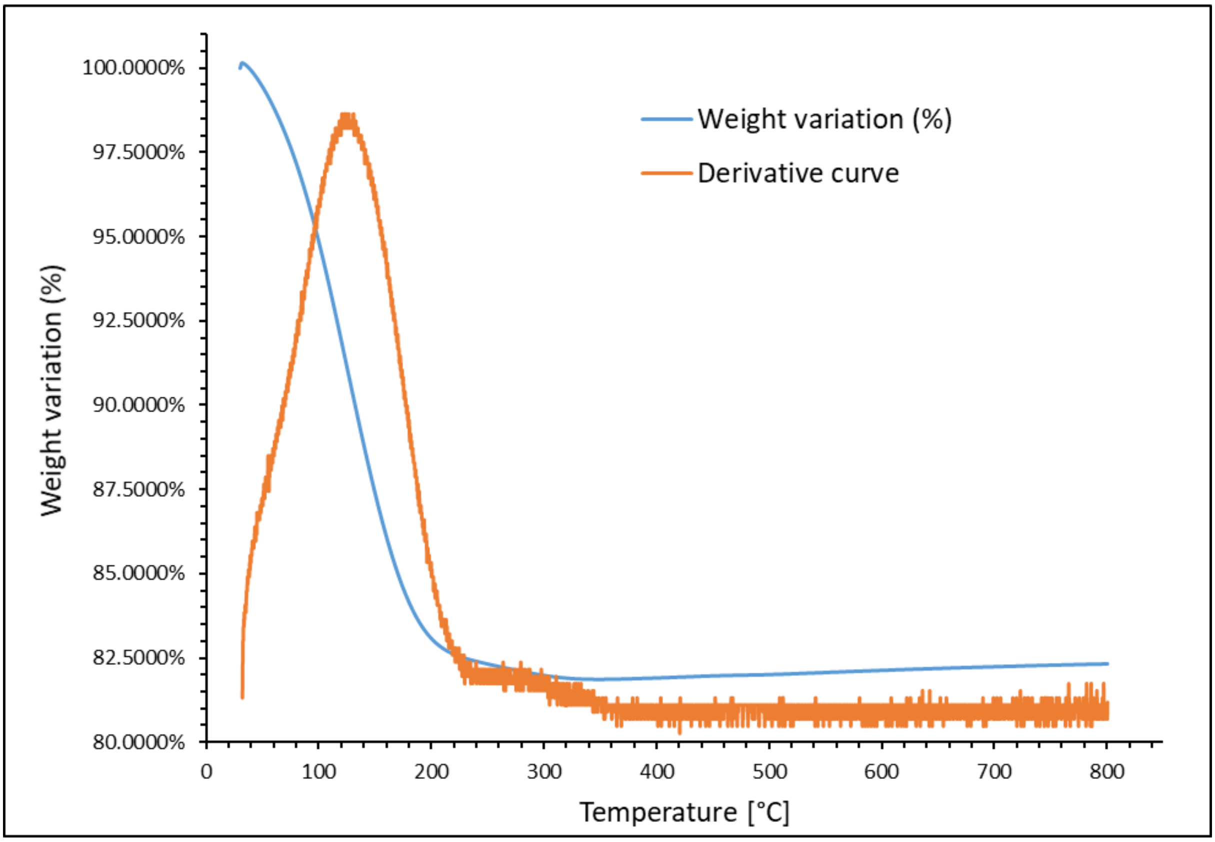

Figure S6: Rietveld plot of nano faujasite K-Y dehydrated in situ on beam line ID22 at ESRF (λ = 0.354417 (1) Å). The angular ranges 12.4-26.4° and 26.4-40° in 2θ (°) are magnified by factors 80 and 500, respectively.

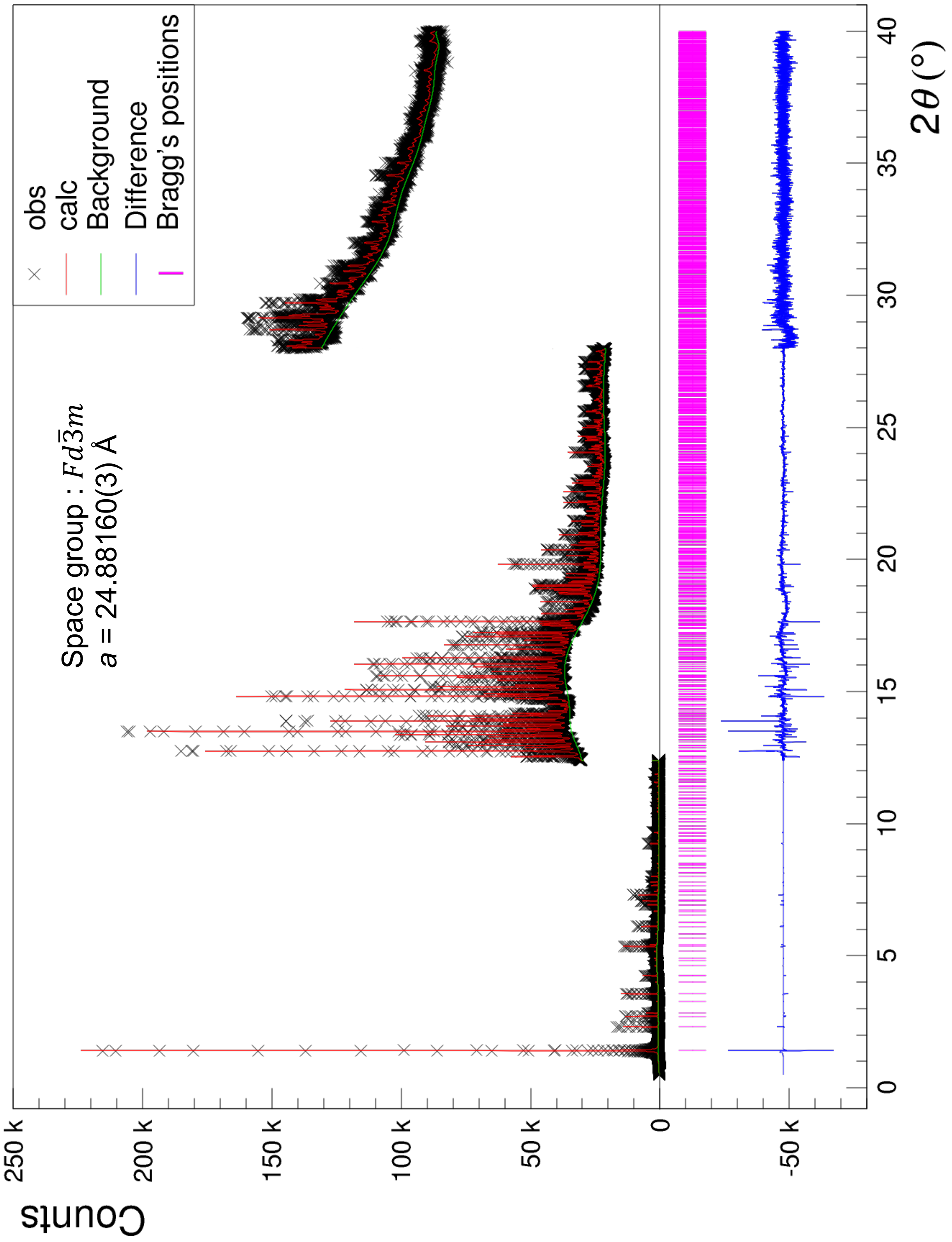

Figure S7: Snapshots of the MC simulation results showing the loadings of 45 (top) and 100 (bottom) H_2O/u.c. in nano-faujasite K-Y. The yellow, orange, red, and cyan spheres represent silicon, aluminum, bridging oxygen atoms of the zeolite framework, and K^+ cations identified in the present 3D ED study, respectively. Blue dots indicate the oxygen atoms of water molecules, while cyan dots correspond to K^+ cations locations identified by simulations.